⌘ *Author's Choice*

THE JOURNAL OF BIOLOGICAL CHEMISTRY VOL. 283, NO. 52, pp. 36234–36240, December 26, 2008

Eag1 Expression Interferes with Hypoxia Homeostasis and Induces Angiogenesis in Tumors*[S]

Received for publication, March 6, 2008, and in revised form, September 19, 2008 Published, JBC Papers in Press, October 16, 2008, DOI 10.1074/jbc.M801830200

Bryan R. Downie[‡], Araceli Sánchez[‡], Hendrik Knötgen[§], Constanza Contreras-Jurado[‡], Marco Gymnopoulos[§], Claudia Weber[‡], Walter Stühmer[‡], and Luis A. Pardo[‡§1]

From the [‡]Max-Planck Institute of Experimental Medicine, Hermann-Rein Str. 3, 37075 Göttingen, Germany and [§]iOnGen AG, Stiegbreite 13, 37077 Göttingen, Germany

Ether-á-go-go-1 (Eag1) is a CNS-localized voltage-gated potassium channel that is found ectopically expressed in a majority of extracranial solid tumors. While circumstantial evidence linking Eag1 to tumor biology has been well established, the mechanisms by which the channel contributes to tumor progression remain elusive. In this study, we have used *in vivo* and *in vitro* techniques to identify a candidate mechanism. A mutation that eliminates ion permeation fails to completely abolish xenograft tumor formation by transfected cells, indicating that Eag1 contributes to tumor progression independently of its primary function as an ion channel. Our data suggest that Eag1 interferes with the cellular mechanism for maintaining oxygen homeostasis, increasing HIF-1 activity, and thereby VEGF secretion and tumor vascularization.

Ether-à-go-go 1 (Eag1,[2] *KCNH1*, Kv10.1 (1)) is the founding member of the *eag* voltage-dependent potassium channel family, which also includes Erg and Elk channels (2, 3). The human Eag1 is normally expressed only within the nervous system (4, 5), yet ectopic Eag1 expression has been increasingly linked to oncogenesis and tumor progression. Overexpressing Eag1 induces a phenotype with characteristic features of tumorigenic cells (5). Additionally, Eag1 mRNA and its product have been detected in numerous cancer cell lines (6–8) and primary tumors (9–11). Finally, siRNA-mediated knockdown of Eag1 expression reduces proliferation (12), and the inhibition of channel function reduces tumor progression both *in vitro* (7, 13) and *in vivo* (14). Yet despite the clear involvement of Eag1 in proliferation and tumor progression, the mechanism of its transformative properties has remained a mystery.

Several other K^+ channels have been implicated in tumor progression and cell proliferation (15–17). Different theories have attempted to explain the possible role of potassium channels in proliferation, all of which rely on the effects of increased potassium permeability (*e.g.* Refs. 18–20). Despite these efforts, a clear relationship between potassium permeation and tumor progression has yet to be established. In particular, the reason why only some channels can influence the behavior of tumor cells remains elusive (15–17, 21).

In this study, we investigated a possible interaction between Eag1 and signaling routes known to be relevant for tumor progression. The hypoxic intratumoral environment promotes the activation of hypoxia-inducible factor 1 (HIF-1), which is a key transcription factor influencing a broad spectrum of functions. Among them, neo-vascularization through transcriptional activation of vascular endothelial growth factor (VEGF) has become a promising target for cancer therapy as neoangiogenesis has a major influence on tumor progression (*e.g.* Ref. 22). In the presence of normal oxygen conditions, the regulated subunit of HIF-1 (HIF-1α; Refs. 23, 24) is rapidly degraded by the proteasome on an order of minutes (25) in an ubiquitin-dependent manner. The E3 ubiquitin ligase responsible for this process contains pVHL (von-Hippel-Lindau tumor suppressing factor), a well-established tumor suppressor (26). Previous reports show an influence of pVHL in the functional expression of Eag1 in neuroblastoma cells (27), which was interpreted as a sign for differentiation to a neuronal phenotype. We designed the present study to elucidate a possible cross-talk between Eag1 and the hypoxia homeostasis system.

EXPERIMENTAL PROCEDURES

Cell Culture—All parental cell lines were obtained from DSMZ (Germany) and maintained according to the instructions of the provider. Transient transfections were performed using Fugene (Roche Applied Science). Stable transfectants were selected and maintained using Zeocin (Calya, 3 μg/ml in culture medium). 24 h after transfection, transiently transfected cells were transferred to hypoxic conditions for 4 h. Culturing under hypoxia was performed by N_2 injection in an oxygen-controlling chamber (Labotec).

Flow Cytometry—Cells were incubated for 20 h in the absence of selective pressure, washed twice with cold PBS, and fixed for 30 min with 4% *p*-formaldehyde at 4 °C. Fixed cells were scraped from the flask, washed three times, and permeabilized with 0.3% saponin for 15 min at room temperature. Cells were then incubated with 10% bovine serum albumin, 0.15% saponin for 15 min to block nonspecific binding, and incubated for 2 h at 4 °C with HIF-1a antibody (AB463, BD Biosciences) diluted 1:100 in 0.1% saponin/2% bovine serum albumin in PBS (PBS-SB). Cells were washed three times with PBS-SB and then incubated 1.5 h with a Cy5-conjugated anti-mouse antibody diluted 1:5000 in PBS-SB.

* The costs of publication of this article were defrayed in part by the payment of page charges. This article must therefore be hereby marked "*advertisement*" in accordance with 18 U.S.C. Section 1734 solely to indicate this fact.
⌘ *Author's Choice*—Final version full access.
[S] The on-line version of this article (available at http://www.jbc.org) contains supplemental information.
[1] To whom correspondence should be addressed. Tel.: 495513899643; Fax: 495513899644.
[2] The abbreviations used are: Eag, ether-à-go-go; PBS, phosphate-buffered saline; VEGF, vascular endothelial growth factor; ELISA, enzyme-linked immunosorbent assay; HIF, hypoxia-inducible factor.

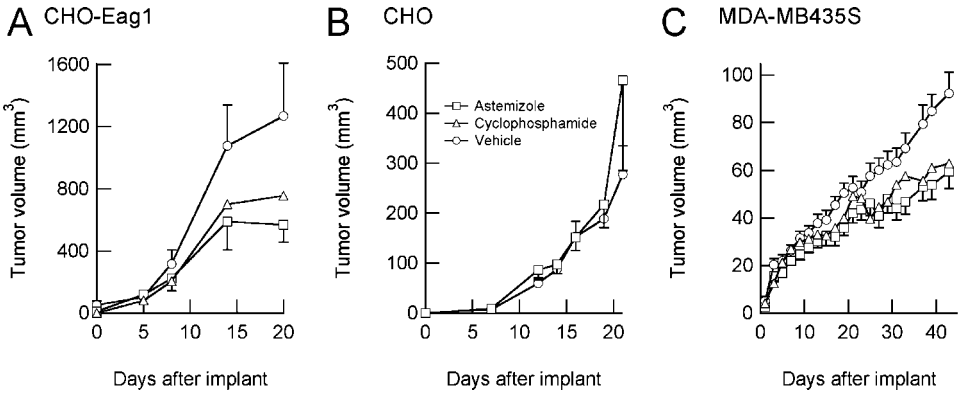

FIGURE 1. **Block of Eag1 by astemizole inhibits tumor growth *in vivo* in an Eag1-dependent way.** Daily oral administration of astemizole (□) reduced the growth rate of xenograft tumors induced by implantation of Eag1-transfected CHO cells with respect to vehicle-treated controls (○) (*A*), but failed to inhibit the growth of tumors induced by wild-type CHO cells (*B*). *C*, breast cancer xenograft model cell line MDA-MB435S, which natively expresses Eag1, exhibits a reduction of tumor growth when animals were treated with astemizole. The extent of the astemizole effect was comparable with the well-established cytotoxic drug cyclophosphamide (△).

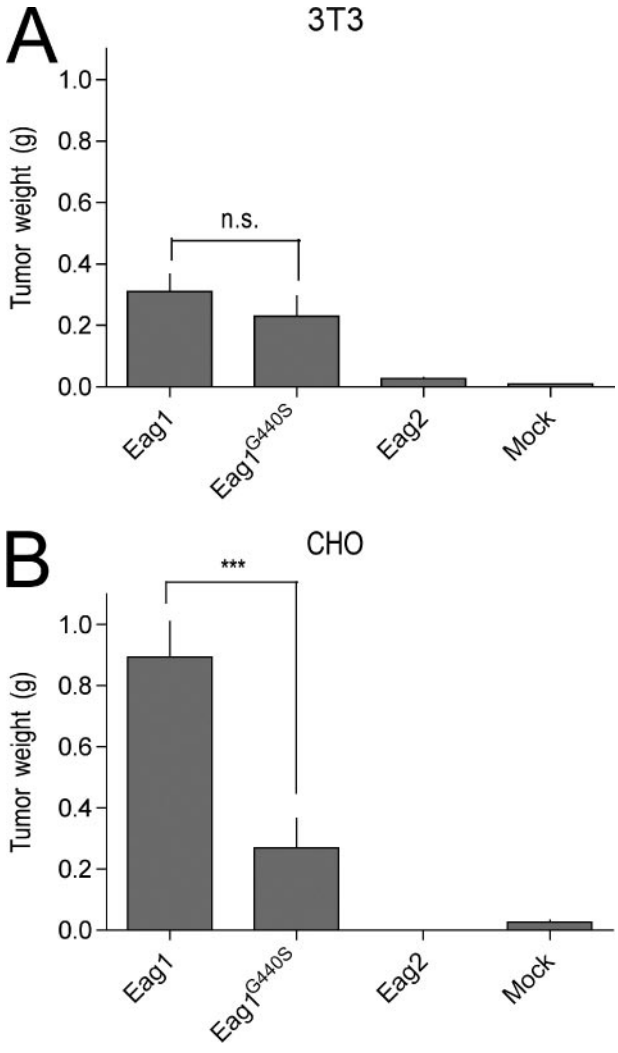

FIGURE 2. **Eag1-G440S-expressing cells form tumors.** *A*, tumor weight comparisons between xenografted Eag1-wt ($n = 9$), Eag1-G440S ($n = 10$), Eag2-wt ($n = 10$), or vector-transfected ($n = 10$) NIH3T3 cells. Eag1-G440S-expressing cells statistically equivalent tumors as Eag1-transfected cells ($p = 0.3$). *B*, CHO cells transfected with Eag1- ($n = 16$), Eag1-G440S ($n = 16$), Eag2- ($n = 15$), or vector ($n = 5$) show similar behavior, albeit G440S-expressing tumors are significantly smaller. *n.s.*, nonsignificant; ***, $p < 0.001$.

Cells were again washed three times and assessed for Cy5 fluorescence using a BD FACSAria flow cytometer (Becton Dickinson, Heidelberg, Germany) with 633-nm laser excitation. Forward and side scatter were used to detect and discard cell fragments and doublets. Data are presented as average fluorescence.

VEGF ELISA—Mock-transfected, Clone A, Clone B, and Clone C HEK293 cells were counted and plated at the same density in 25 cm^2 flasks. Cells were cultured overnight with medium containing the selective agent Zeocin (3 μg/ml), after which the media was changed and cultured for 20 h without selection pressure. Cell culture supernatant was removed and centrifuged to remove cell particulates and detached cells, then assayed for secreted VEGF (Quantikine VEGF ELISA assay kit, R&D Systems). Cells in the flask were stained with propidium iodide and counted using a flow cytometer.

Luciferase Assay—Mock-transfected and Clone A cells were counted and plated at the same density in 6-well plates. Cells were then transfected using Lipofectamine 2000 in Optimem with Bartrons HRE vector for 4 h, after which the medium was changed to normal growth medium. Luminescence was assayed using a Luciferase Reporter Gene Assay from Roche Applied Science.

Western Blot—For HIF1α detection, cells were lysed in 10 mM Tris-HCl pH 6.8, 1% SDS, 5 mM dithiothreitol, Protease Inhibitor Mixture (Roche Applied Science), and 8 M urea and to minimize HIF degradation, homogenized using an UltraTurrax device, centrifuged (14,000 $\times$ *g* 15 min), and the supernatant was used as total cell extract. Protein concentration was determined using BCA (Pierce).

Protein extracts were separated by gradient SDS-PAGE (either 3–8 or 4–12%) and transferred to nitrocellulose membranes. Membranes were blocked with 0.1% casein (Roche Applied Science) and incubated with the corresponding antibody. Antibody against HIF1α (BD Transduction Laboratories) was used at 0.5–1 μg/ml overnight in a humidified chamber. After washing and incubation with appropriate peroxidase-labeled secondary antibody, blots were developed using Millipore Immobilon system. Signals were detected in a Bio-Rad Chem-Doc luminescence detection system.

Mouse Models—MDA-MB-435S (8×10^6), CHO (2×10^6), or NIH3T3 cells (6×10^6) were implanted into the flank of 8-week-old female scid mice (Taconic). End point experiments were carried out for 3 weeks. For tumor growth inhibition experiments, treatment started after the tumors reached a size of 2 mm in diameter, daily via an oral feeder. Astemizole (Sigma) was prepared as stock solution (50 mg/ml) in DMSO and diluted in phosphate-buffered saline prior to administration. As a positive control, 5 mg/kg cyclophosphamide (Sigma) was administered to the animals using the same protocol. Body weight and tumor size (using a caliper) were measured every 2 days. To minimize errors, the same operator always measured

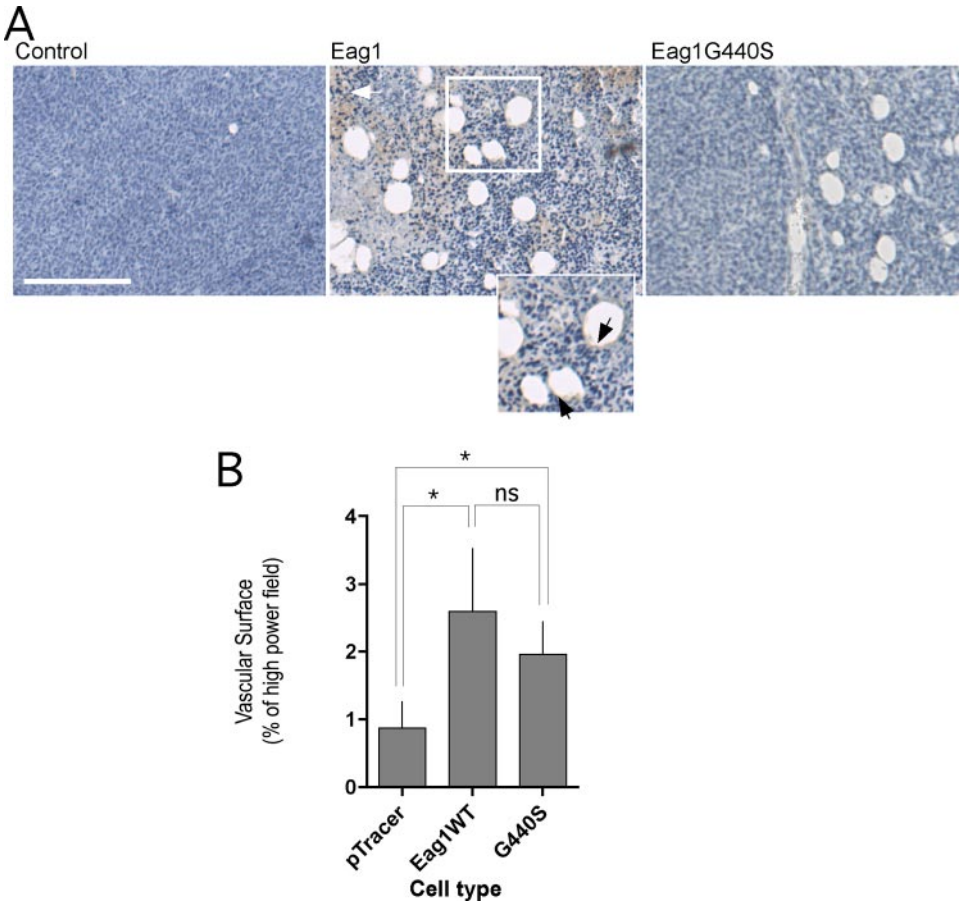

FIGURE 3. **Eag1-expressing tumors display increased vascularization.** *A*, histological appearance of tumors induced by CHO cells in the presence or absence of Eag1 or Eag1 G440S expression. Sections from PFA-fixed and paraffin-embedded tumors from xenografted mock-transfected and Eag1-transfected CHO cells in SCID mice were immunostained for CD31 expression and counterstained with hematoxylin. Endothelial cells were identified by CD31 staining (*Inset*, *arrowheads*; scale bar, 50 μm) Note the prominent necrosis in Eag1-wild type-expressing tumors (*white arrow*), which correlates with the previously described behavior of these implants (5). Tumors of similar sizes were selected for representation. *B*, quantification of the surface occupied by CD31-positive capillaries in the three types of tumors depicted in *A*. Tumors expressing Eag1 and Eag1G440S showed significantly increased vascularization (mean $\pm$ S.E.; *, $p < 0.05$).

the tumors. Tumor weight was determined *ex vivo* at the end of the experiment.

Immunohistochemistry—Formalin-fixed and paraffin-embedded tumor sections were deparaffinized and rehydrated in a series of xylol and ethanol solutions. Antigen retrieval was performed in a microwave oven in 10 mM citrate buffer (pH 6.0) for 15 min. Slides were incubated overnight in a humidified chamber at 4 °C with anti CD34, anti VEGF receptor, anti-Factor VIII (all from Abcam) or anti-CD31 antibodies (Santa Cruz Biotechnology) and immunoreactivity was detected using the Envision Peroxidase System and DAB (DAKO). Sections were counterstained with hematoxylin and thereafter dehydrated and mounted in xylol-based mounting medium. The quantification of vascular surface was performed by a blinded operator using ImageJ software on 25 high power fields (400×) from each sample acquired.

RESULTS

Open Channel Blockade of Eag1 Channels Reduces Tumor Progression in Vivo—Because inhibition of Eag1 by the open channel blockers astemizole and imipramine has been reported to inhibit proliferation of several cell types *in vitro* (7, 13), we tested if similar effects could be observed *in vivo*. CHO cells expressing Eag1 were implanted into SCID mice and astemizole (50 mg/kg) administered daily via oral gavage once palpable tumors had developed. Astemizole was selected instead of imipramine as it does not pass the blood-brain barrier and should therefore have little effect on intracranial Eag1. Tumor growth induced by implantation of Eag1-expressing cells was clearly inhibited in the group treated with astemizole (Fig. 1*A*), similar to growth inhibition observed after treatment with the well-established cytotoxic drug cyclophosphamide (CPM) (applied at the maximal tolerable dose of 5 mg/kg). The antitumoral effect of astemizole can be at least partially attributed to Eag1 blockade, as no growth inhibition occurred after application of astemizole in wild-type CHO cell tumors (Fig. 1*B*).

We subsequently tested the effect of astemizole on the slowly growing human cancer xenograft model MDA-MB435S. This cell line expresses Eag1, but not HERG (a relative of Eag1 that is very effectively blocked by astemizole and has also been implicated in tumor progression (28)). Astemizole was again able to inhibit tumor progression nearly as effectively as cyclophosphamide (Fig. 1*C*) without noticeable toxic effects. These results indicate that reducing ion permeation through Eag1 reduces tumor progression *in vivo*, in good agreement with results reported using a specific anti-Eag1 antibody (14).

Eliminating Ion Permeation Does Not Abolish Tumor Formation by Xenografted NIH3T3 Cells in Vivo—This effect of astemizole may indicate that potassium permeation is required for Eag1 to favor tumor growth. If potassium permeation is the only feature of Eag1 channels relevant to tumor progression, elimination of ion permeation (through a point mutation in the pore region) should also abolish Eag1-induced tumor progression *in vivo*. For these experiments NIH3T3 and CHO cells were used as xenograft models. Wild-type or mock-transfected NIH3T3 cells induce no tumors when implanted into SCID mice, while Eag1-expressing cells do. Previous experiments demonstrated that tumors arising from the implantation of Eag1-transfected CHO cells into SCID mice are larger and more aggressive than those generated by wild-type CHO cells (5).

Ion permeation was abolished by mutating a glycine residue in the signature sequence of the pore region (MTSVGF*G*N) to

serine (G440S). This strategy has already been successfully applied to several ion channels, including Eag family members (29). To verify that the protein was synthesized and functional, RNA encoding the mutant channel was injected into *Xenopus* oocytes and electrophysiologically characterized. Although not permeating ions, correctly assembled and membrane resident channels should respond to membrane depolarizations by conformational changes that can be detected as capacitive currents (gating currents) by electrophysiological techniques. Expression of Eag1-G440S channels gave rise to gating currents with properties compatible with Eag1 (see supplemental information).

Stable polyclonal NIH3T3 and CHO transfectants of the G440S mutant were implanted subcutaneously in the flank of female SCID mice. While previous experiments have shown that neither wild type nor vector-transfected NIH3T3 cells give rise to tumors in this system, G440S cells were found to produce tumors, albeit reduced in weight compared with wild-type Eag1 tumors (Fig. 2*A*). Therefore, ion permeation influences the oncogenic properties of Eag1, but it is not an absolute requirement. Comparable results were obtained when CHO cells were used (Fig. 2*B*) in two different strains of SCID mice (CB17 and scid/beige). G440S mutant channels induced tumors noticeably smaller than wild-type Eag1, but larger than mock- or Eag2-transfected cells. It is important to note that as an open channel blocker, astemizole locks the channel in the open conformation, while the G440S mutant can still undergo conformational transitions during gating.

Eag1-expressing Tumors Show Increased Angiogenesis—In contrast to NIH3T3 cells, non-transfected CHO cells also form sizeable tumors. This allows a direct comparison of the structure of tumors derived from Eag1-positive and Eag1-negative cells. Structures morphologically compatible with blood vessels were observed in tumors of similar volume arising from wild-type or mock-transfected cells, but the frequency of these was greatly increased in tumors expressing Eag1 (Fig. 3*A*). Positive staining with the well-established endothelial marker CD31 (Fig. 3*A*, *arrows inset*) indicates the presence of endothelial cells and thus identifies the structures as capillaries, indicating that Eag1 expression favors the formation of vascular structures in tumors. Eag1 G440S expression induced similar morphologies in xenograft tumors (Fig. 3*A*, *right*), indicating that increased vascularization does not require potassium permeation.

Quantification of vascularization by measurement of CD31, VEGF-R, or Factor VIII-positive structures (*i.e.* capillaries) in 25 high power fields from at least two tumors of each type confirmed increased vascular structure surface area in both Eag1 and Eag1 G440S-expressing tumors (Fig. 3*B*).

In light of these data, a possible explanation for the retained tumorigenic ability of mutant permeation-deficient Eag1 channels could be increased vascularization in these tumors. This observation further supports the idea that to some degree the transformative properties of Eag1 are independent of its canonical function as an ion channel and may be instead dependent on an interference with the cellular oxygen homeostasis system. More abundant vascularization would increase oxygen and nutrient supply to tumor cells and represent a selective growth advantage for Eag1-expressing cells.

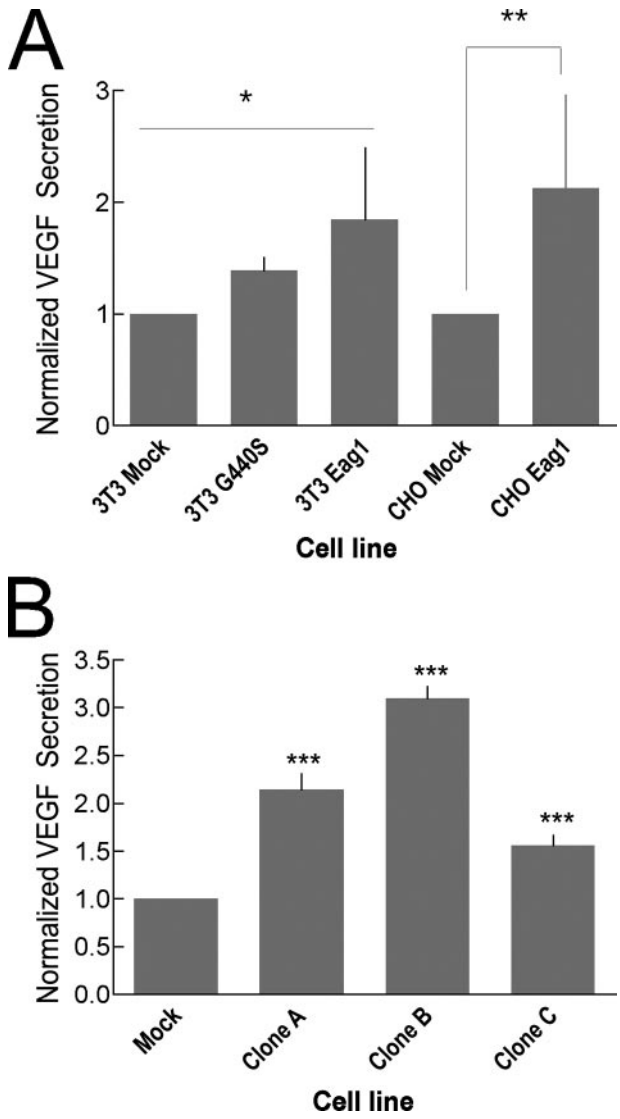

FIGURE 4. **Eag1 expression induces increased VEGF secretion.** *A*, VEGF is more abundant in the cell culture supernatant of polyclonal stably transfected NIH3T3 expressing the human Eag1 or Eag1 G440S. CHO cells expressing Eag1 also show increased VEGF secretion over mock-transfected. The *asterisks* indicate statistical significance by analysis of variance (3T3, $p < 0.05$) or Student's *t* test (CHO, $p < 0.01$). *B*, compared with mock-transfected cells, Eag1-expressing clones A, B, and C all exhibit greatly increased secretion of VEGF ($p < 0.0001$, Student's *t* test) as measured by ELISA.

Eag1 Expression Promotes VEGF Secretion in Vitro—Among the many factors influencing angiogenesis, VEGF appears to be predominant (30, 31). VEGF has drawn intense attention in the field of oncology due both to its influence on tumor survival and to its potential use in cancer therapies. To test the possibility that the observed increase in vascularization of Eag1-expressing tumors correlates to an increase in secreted VEGF, we determined VEGF abundance in the culture supernatant of cells expressing Eag1. Determinations on the cell lines used for xenograft experiments showed (Fig. 4*A*) increased VEGF secretion in cells expressing both Eag1 and Eag1G440S.

Commercially available antibodies and kits for the determination of VEGF are normally targeted to the human factor. These kits provide much better sensitivity and reproducibility

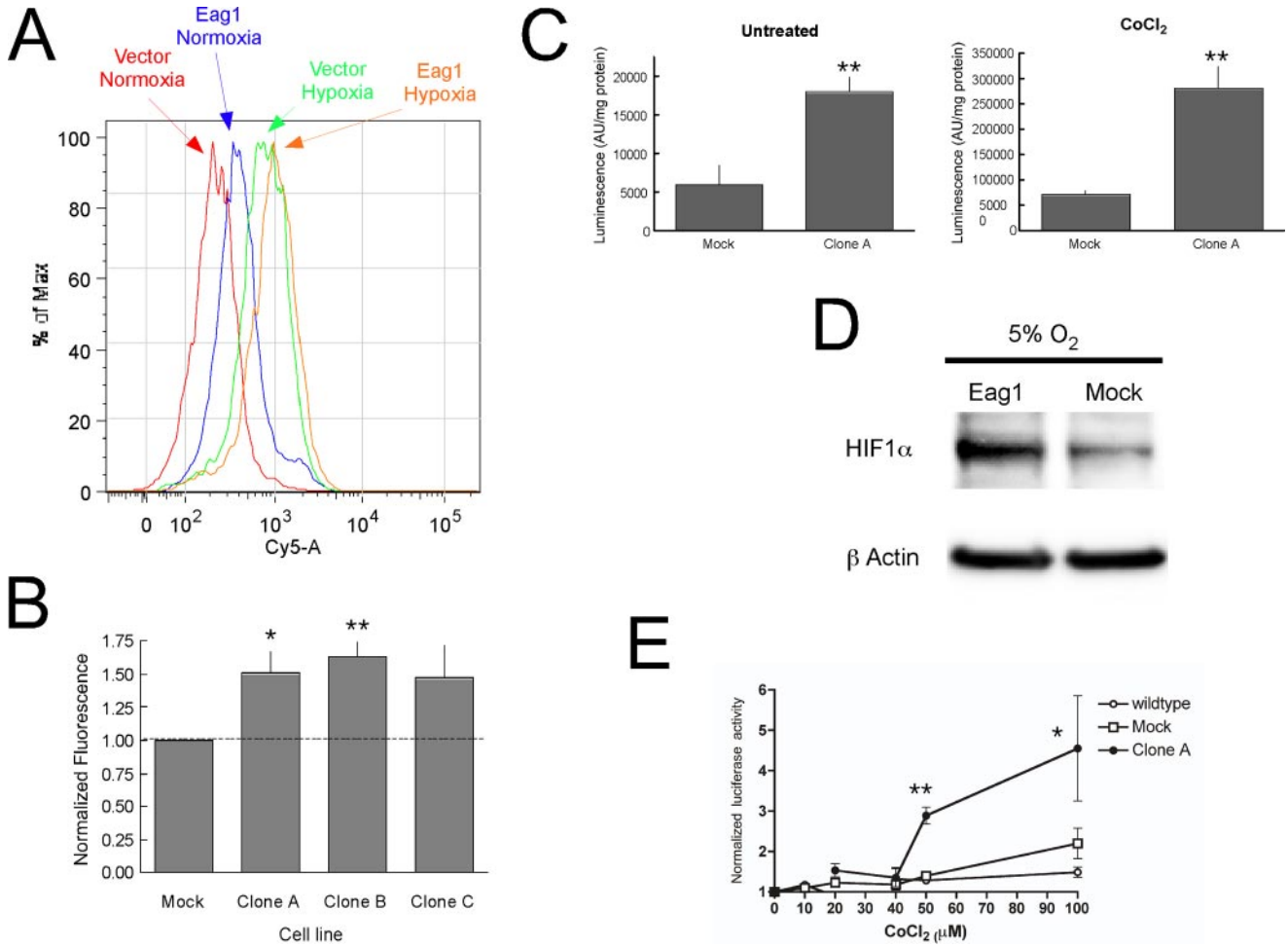

FIGURE 5. **HIF-1α protein is increased in Eag1-expressing cells.** *A*, representative peak shift of HIF-1α fluorescence in flow cytometry experiments using anti-HIF-1α antibodies and Cy5.5-labeled secondary antibody on Eag1-transfected as compared with mock-transfected cells under normoxic (21% O_2) or hypoxic (1% O_2 for 4 h) conditions. *B*, quantitative HIF-1α fluorescence increase in Clones A, B, and C over mock-transfected. *C*, Eag1-expressing cells show increased HRE-dependent luciferase activity over mock-transfected cells in both untreated and $CoCl_2$-treated cultures. *D*, HIF-1α is more abundant in Eag1-transfected cells when incubated under mild hypoxia (5% O_2). *E*, HRE activity is elicited by lower $CoCl_2$ concentrations in Eag1-expressing cells. Luciferase activity is represented normalized for activity in the absence of $CoCl_2$. *, $p < 0.05$; **, $p < 0.01$.

on human samples and so HEK293 cells were selected for their human origin and ease-of-use.

To discard artifacts due to genomic insertion, VEGF secretion was measured in three independent clones of the HEK293 cell line stably expressing Eag1 by ELISA (Clones A, B, and C) and compared with mock-transfected cells. All three Eag1-expressing cell lines were found to secrete significantly more VEGF than the non-transfected control (Fig. 4*B*). This VEGF increase correlates with the observed vascularization increase of Eag1-expressing tumors.

Eag1 Increases HIF-1α—The most likely candidate for the up-regulation of VEGF in Eag1-transfected cells and increase in vascularization in Eag1-expressing tumors is a functional increase of HIF-1. To investigate this possibility, HIF-1α expression was examined using flow cytometry for HEK293 Clones A, B, and C with an anti-HIF-1α antibody and a fluorescently labeled (Cy5.5) secondary antibody. Compared with mock-transfected cells, the fluorescence histogram of each clone showed a rightward shift, consistent with an increase in HIF-1α content (Fig. 5*A*). The peak shift induced by Eag1 expression was much less intense under hypoxia. Quantitative comparison of the mean HIF-1α fluorescence values calculated for each cell line and normalized to mock-transfected cells is shown in Fig. 5*B*. Each clone displayed independently of oxygen concentration and culture conditions (data not shown) modest but significantly increased HIF-1α fluorescence over mock-transfected cells.

To test whether this increase of HIF-1α can have functional implications, we studied the activity of a HIF-1 responsive promoter. This was done by determining the luciferase activity in both control and Eag1-expressing HEK293 cells transiently transfected with a reporter vector encoding luciferase under control of the HRE of 6-phosphofructo-2-kinase (HRE-Luc) (32). Eag1-expressing cells (Clone A) maintained in normoxia showed a dramatic increase in luciferase activity compared with control cells after 48 h (Fig. 5*C*, *left panel*). Mock-hypoxic conditions induced by 200 μM $CoCl_2$ treatment for 18 h resulted in luciferase activity increases in both control and transfected cells, while maintaining a similar increase in Eag1-expressing cells (Fig. 5*C*, *right*).

Western blot analysis of cell extracts from cultures exposed to either 21 or 1% O_2 did not consistently show increases in

HIF-1α protein content. However, mild hypoxia (5% O_2, 4 h; Fig. 5*D*) induced a clear increase in HIF1α abundance in Eag1-expressing cells. Because no increase in HIF was observed under normoxia, it is unlikely that the differences in HIF abundance can be attributed to an artifactual local hypoxia. A comparable elevation in HIF1α content was observed in transiently transfected cells when hypoxia (7% O_2, 4 h) was applied 24 h after transfection (not shown).

These results indicate that Eag1 expression induces an increase in HIF1α under mild hypoxia, which could reflect a shift on the threshold of the HIF-1 system. To investigate this, we determined the increase of HIF-1α activity over basal conditions in the presence of different concentrations of Co^{2+} in Eag1 and mock-transfected cells. Eag1-expressing cells were found to induce increased HIF-1α activity at lower concentrations of Co^{2+} (Fig. 5*E*). This finding could be interpreted as the result of interference of Eag1 with the HIF-1α control pathway. Altogether, these results suggest a causal relationship between the functional increase in HIF-1α and the increase of VEGF secretion observed in Eag1-expressing cell lines.

DISCUSSION

Despite several studies implicating ectopic expression of Eag1 in many cancer cell lines and primary tumors (5, 7–12, 21), information regarding the mechanism of Eag1 contribution to oncogenesis has thus far remained unclear. Using a broad spectrum of techniques, we present evidence indicating that the oncogenic potential of Eag1 is partly independent of its primary physiological function as an ion channel. We also show a functional up-regulation of HIF-1 and VEGF in Eag1-expressing cells. We propose a possible mechanism by which Eag1 could favor tumor progression through increased angiogenesis under the characteristic hypoxia of tumor microenvironment.

Eag1 inhibition has proven efficacious in reducing tumor cell proliferation *in vitro*. However, a point mutation in Eag1 that abolishes ion permeation failed to eliminate tumor induction in NIH3T3 cells *in vivo*. This observation strongly suggests that ion permeation is not essential for the tumor promoting activity of Eag1. While at first seeming incompatible with the reported ability of a functional antibody to inhibit tumor progression (14), this result would be explained if the conformational changes normally accompanying gating constitute a significant part of the Eag1 tumorigenic signal; a blocked channel would be locked in a defined conformational state, whereas the mutant channel would still be able to undergo conformational changes. Therefore, properties of Eag1 other than ion permeation must influence cellular signaling, as has recently been proposed for *Drosophila* eag (33) and other voltage-gated channels (34).

The very high frequency of ectopic expression of Eag1 in primary tumors (9, 10) indicates that Eag1 expression confers a selective advantage to tumor cells under conditions that are common to the majority of neoplasms. Such a common condition could be hypoxia. The major immediate consequence of hypoxia is HIF-1 up-regulation, which is widely accepted as a hallmark of cancer physiology, both from our understanding of the tumor microenvironment and the role of HIF-1 target genes in cell proliferation, survival and angiogenesis (35). Interestingly, mutations of both Eag1 and HIF prolyl-hydroxylase orthologs in *Caenorhabditis elegans* result in a similar egg-laying defect phenotype (reviewed in Ref. 36).

The observed increase in HIF-1 activity in Eag1-expressing cells represents a novel explanation for the oncogenic potential of Eag1. The ectopic expression of Eag1 could thus have far reaching effects, as the increased secretion of growth factors and angiogenic-signaling molecules such as VEGF would have lasting effects within the local tumor microenvironment. Recently it has been reported that the related channel HERG also influences VEGF secretion in glioblastoma cell lines, although the mechanism by which this is achieved remains unclear (37). Murata *et al.* (27) described a negative correlation between pVHL and functional Eag1 expression. It is tempting to speculate that this interaction between the factor in charge of controlling the levels of HIF1 and Eag1 underlies the observed increase in HIF1 under mild hypoxia in Eag1-expressing cells, although this hypothesis requires direct testing.

In summary, we have observed in this study a novel non-canonical contribution of an ion channel to tumor formation. While non-canonical protein functions have been proposed as relevant for the phenotypic changes induced in heterologous systems (*e.g.* Refs. 38, 39), the evidence presented in this report supports their role in native systems as well.

Acknowledgments—We thank D. A. Brown (UCL), D. Katschinski (University Göttingen), and F. Melchior (University Göttingen) for helpful suggestions, R. Bartrons, and D. Katchinski for the HRE reporter vectors, F. Mello de Queiroz and C. Kleinert for help in some experiments, S. Smith for assistance with editing the manuscript, and V. Díaz-Salamanca for excellent technical assistance.

REFERENCES

1. Gutman, G. A., Chandy, K. G., Grissmer, S., Lazdunski, M., McKinnon, D., Pardo, L. A., Robertson, G. A., Rudy, B., Sanguinetti, M. C., Stühmer, W., and Wang, X. (2005) *Pharmacol. Rev.* **57,** 473–508
2. Bauer, C. K., and Schwarz, J. R. (2001) *J. Membr. Biol* **182,** 1–15
3. Warmke, J. W., and Ganetzki, B. (1994) *Proc. Natl. Acad. Sci. U. S. A.* **91,** 3438–3442
4. Occhiodoro, T., Bernheim, L., Liu, J. H., Bijlenga, P., Sinnreich, M., Bader, C. R., and Fischer-Lougheed, J. (1998) *FEBS Lett.* **434,** 177–182
5. Pardo, L. A., del Camino, D., Sánchez, A., Alves, F., Brüggemann, A., Beckh, S., and Stühmer, W. (1999) *EMBO J.* **18,** 5540–5547
6. Meyer, R., and Heinemann, S. H. (1998) *J. Physiol.* **508,** 49–56
7. Ouadid-Ahidouch, H., Le Bourhis, X., Roudbaraki, M., Toillon, R. A., Delcourt, P., and Prevarskaya, N. (2001) *Recept. Channels* **7,** 345–356
8. Meyer, R., Schonherr, R., Gavrilova-Ruch, O., Wohlrab, W., and Heinemann, S. H. (1999) *J. Membr. Biol.* **171,** 107–115
9. Mello de Queiroz, F., Suarez-Kurtz, G., Stühmer, W., and Pardo, L. A. (2006) *Mol. Cancer* **5,** 42
10. Hemmerlein, B., Weseloh, R. M., Queiroz, F. M. d., Knötgen, H., Sánchez, A., Rubio, M. E., Martin, S., Schliephacke, T., Jenke, M., Heinz-Joachim-Radzun, Stühmer, W., and Pardo, L. A. (2006) *Mol. Cancer* **5,** 41
11. Farias, L. M. B., Bermúdez Ocaña, D., Díaz, L., Larrea, F., Avila-Chávez, E., Cadena, A., Hinojosa, L. M., Lara, G., Villanueva, L. A., Vargas, C., Hernández-Gallegos, E., Camacho-Arroyo, I., Dueñas-González, A., Pérez-Cárdenas, E., Pardo, L. A., Morales, A., Taja-Chayeb, L., Escamilla, J., Sánchez-Peña, C., and Camacho, J. (2004) *Cancer Res.* **64,** 6996–7001
12. Weber, C., Mello de Queiroz, F., Downie, B., Sukow, A., Stühmer, W., and Pardo, L. A. (2006) *J. Biol. Chem.* **281,** 13033–13037
13. Gavrilova-Ruch, O., Schönherr, K., Gessner, G., Schönherr, R., Klapperstuck, T., Wohlrab, W., and Heinemann, S. H. (2002) *J. Membr. Biol.* **188,** 137–149

14. Gomez-Varela, D., Zwick-Wallasch, E., Knotgen, H., Sanchez, A., Hettmann, T., Ossipov, D., Weseloh, R., Contreras-Jurado, C., Rothe, M., Stuhmer, W., and Pardo, L. A. (2007) *Cancer Res.* **67,** 7343–7349
15. Pardo, L. A., Contreras-Jurado, C., Zientkowska, M., Alves, F., and Stuhmer, W. (2005) *J. Membr. Biol.* **205,** 115–124
16. Pardo, L. A. (2004) *Physiology* **19,** 285–292
17. Conti, M. (2004) *J. Exp. Ther. Oncol.* **4,** 161–166
18. Rouzaire-Dubois, B., Malo, M., and Dubois, J. M. (2002) in *Ion Channels and Physiopathologies of Nerve Conduction and Cell Proliferation* (Rouzaire-Dubois, B., Benoit, E., and Dubois, J. M., eds) pp. 187–200, Research Signpost, Trivandrum, India
19. Dubois, J. M., and Rouzaire-Dubois, B. (2004) *Eur. Biophys. J.* **33,** 227–232
20. Wonderlin, W. F., and Strobl, J. S. (1996) *J. Membr. Biol.* **154,** 91–107
21. Stuhmer, W., Alves, F., Hartung, F., Zientkowska, M., and Pardo, L. A. (2006) *FEBS Lett.* **580,** 2850–2852
22. Collins, I., and Workman, P. (2006) *Nat. Chem. Biol.* **2,** 689–700
23. Ivan, M., Kondo, K., Yang, H., Kim, W., Valiando, J., Ohh, M., Salic, A., Asara, J. M., Lane, W. S., and Kaelin, W. G., Jr. (2001) *Science* **292,** 464–468
24. Jaakkola, P., Mole, D. R., Tian, Y. M., Wilson, M. I., Gielbert, J., Gaskell, S. J., Kriegsheim, A., Hebestreit, H. F., Mukherji, M., Schofield, C. J., Maxwell, P. H., Pugh, C. W., and Ratcliffe, P. J. (2001) *Science* **292,** 468–472
25. Maxwell, P. H., Wiesener, M. S., Chang, G. W., Clifford, S. C., Vaux, E. C., Cockman, M. E., Wykoff, C. C., Pugh, C. W., Maher, E. R., and Ratcliffe, P. J. (1999) *Nature* **399,** 271–275
26. Kaelin, W. G., Jr. (2002) *Nat. Rev. Cancer* **2,** 673–682
27. Murata, H., Tajima, N., Nagashima, Y., Yao, M., Baba, M., Goto, M., Kawamoto, S., Yamamoto, I., Okuda, K., and Kanno, H. (2002) *Cancer Res.* **62,** 7004–7011
28. Arcangeli, A. (2005) *Novartis Found Symp.* **266,** 225–232; discussion 232–224
29. Schonherr, R., Gessner, G., Lober, K., and Heinemann, S. H. (2002) *FEBS Lett.* **514,** 204–208
30. Kim, K. J., Li, B., Winer, J., Armanini, M., Gillett, N., Phillips, H. S., and Ferrara, N. (1993) *Nature* **362,** 841–844
31. Millauer, B., Shawver, L. K., Plate, K. H., Risau, W., and Ullrich, A. (1994) *Nature* **367,** 576–579
32. Obach, M., Navarro-Sabaté, A. J. C., Kong, X., Duran, J., Gómez, M., Perales, J. C., Ventura, F., Rosa, J. L., and Bartrons, R. (2004) *J. Biol. Chem.* **279,** 53562–53570
33. Hegle, A. P., Marble, D. D., and Wilson, G. F. (2006) *Proc. Natl. Acad. Sci. U. S. A.* **103,** 2886–2891
34. Kaczmarek, L. K. (2006) *Nat. Rev. Neurosci.* **7,** 761–771
35. Pouyssegur, J., Dayan, F., and Mazure, N. M. (2006) *Nature* **441,** 437–443
36. Schafer, W. R. (2006) *Annu. Rev. Genet.* **40,** 487–509
37. Masi, A., Becchetti, A., Restano-Cassulini, R., Polvani, S., Hofmann, G., Buccoliero, A. M., Paglierani, M., Pollo, B., Taddei, G. L., Gallina, P., Di Lorenzo, N., Franceschetti, S., Wanke, E., and Arcangeli, A. (2005) *Br. J. Cancer* **93,** 781–792
38. Li, Y. M., Zhou, B. P., Deng, J., Pan, Y., Hay, N., and Hung, M. C. (2005) *Cancer Res.* **65,** 3257–3263
39. Tomlinson, V. A., Newbery, H. J., Wray, N. R., Jackson, J., Larionov, A., Miller, W. R., Dixon, J. M., and Abbott, C. M. (2005) *BMC Cancer* **5,** 113